RSC Advances

ROYAL SOCIETY OF CHEMISTRY

www.rsc.org/advances

De novo synthesis of novel bacteriogenic nanocell particles and its cancer cell compatibility evaluation

Muthu Manikandan[1] D. Ramachandaran[2] and Sechul Chun[1*]

[1]Department of Bioresource and Food Science, Konkuk University, Seoul 143-701, Korea

[2]Centre for Nanoscience & Nanotechnology, Sathyabama University, Chennai-600119, India

Corresponding author, Phone: 822-450-3727; e-mail: scchun@konkuk.ac.kr

Abstract

This study demonstrates the effective synthesis of nanocell particles of bacterial origin using the eco-friendly ultrasonic approach. The synthesized particles were separated by sequential centrifugation. The probe sonication technique, with 5 min sonication time at 20 kHz frequency successfully yielded regular spherical shaped organic nanoparticles directly from bacterial biomass in the 33-42nm size regime. The holding capacity of the particles was verified by synthesizing the particles in the presence of acridine orange (AO) and further characterized using FTIR and fluorescence spectroscopy. The internalization ability of all the three different sized particles separated after sonication by differential centrifugation was elaborately investigated on Hela cells using confocal laser scanning microscopy. Out of the three different particles tested, the nanosized particles exhibited maximum internalization capacity. The toxicity/biocompatibility on Hela cancer cells was studied using MTT assay and the results substantiated that all the particles were highly biocompatible. The results confirm that the indigenously synthesized nanocell particles can be used as efficient drug carriers for drug delivery for cancer cells.

Key words: Nanoparticles, ultrasonication, directly, bacterial biomass, facile, ecofriendly

Introduction

Nano sized materials that result from the reduction of their bulk counterparts have been found to have enormous advantages due to their unique physical and chemical properties. Due to their superior characteristics, nanomaterials have been tremendously utilized for technological advancement in almost every other field including: biomedicine, agriculture, food, environment, optics, electronics, magnetics, mechanics, catalysis, energy science and space science. Nanomaterial based technological realm benefits the human society in multiple ways both directly and indirectly[1,2]. Of the various nanomaterials, zero-dimensional nanomaterials are often being used directly for biomedical and consumer products because they resemble the dimension of nanosized protein and other molecules[3-5]. Further the nanosize (<100nm) of the nanoparticles not only offers them superior escape strategies across vital human organs such as lungs, spleen and liver, but also ensures their increased bioavailability in the blood stream and thus makes them unique candidates for efficient treatments with less side effects[6]. In addition to this, the smaller size of the particles enables them to access the cellular milieu without causing too much interference[6].

Nanoparticles have become unavoidable tools in various fields of biomedical research and applications due to their rapid and simple synthesis methods and their uncomplicated chemical manipulations for unique composition[7]. Therefore their application have diverged into various biological and biomedical research aspects like fluorescent biological labelling[8-10], drug and gene delivery[11,12] , detection of pathogens[13], detection of proteins [14], probing of DNA structure[15], tissue engineering [16,17], tumour destruction via heating, hyperthermia [18,19], separation and

purification of biological molecules and cells[20], MRI contrast enhancement[21] and phagokinetic studies[22].

Metal and metal oxide nanoparticles have made a tremendous contribution in medical applications. However their synthesis procedure is complex because their size distribution, shape, metal doping, intrinsic and surface properties mostly rely on their synthesis routes[23]. They also demand excessive use of various chemicals. For the synthesis of various metallic nanoparticles, different wet chemical methods have been adopted with most common reducing agents such as sodium citrate[24] or $NaBH_4$[25], poly(ethylene glycol) (PEG) [26] and common sugars such as glucose, fructose and sucrose[27]. The metal oxide nanoparticles have been synthesized by any one of the following methods: (1) *Co-precipitation method* by which of the metal nanoparticles are precipitated from their salt precursors using bases (NaOH, NH_4OH etc)[28,29]. (2) *Microemulsion method:* which involves the use of micelles during the reaction by which the monodispersed metal oxide nanoparticles within micelle consisting of homogeneous surface chemistry and monodispersed nano particles are obtained [30, 31]. (3) *Sol-gel Method:* by this method, the nanoparticles have been obtained from metal alkoxides and metal chloride precursor hydrolysis and polycondensation reactions too[32]. (4)-*Solvothermal process:* In this method usually metal complexes are first formed and then decomposed by boiling in an inert atmosphere or in an autoclave with the help of pressure (typically between 1 atm and 10,000 atm) and temperature (100-1000 °C) [33-36]. Microwave was also used as a tool to synthesize nanoparticles for biomedical applications [37,38]. During the synthesis of nanoparticles by the above mentioned methods, the particles may harbor toxic chemical species from the reaction which may impose adverse effects when used for biomedical applications[39]. Quite recently, biogenic synthesis of nanoparticles has proven to be successful for both prokaryotes and eukaryotes because of its

enhanced biocompatibility, leading to their profound usefulness in versatile biological applications[40-43]

Apart from the above methods, ultrasonication has also been established as a vital method for the preparation of various metallic, oragnometallic and organic nanoparticles [44-47]. More recently Han et al.,[48] have demonstrated the efficient synthesis of nanocomposites through ultrasonication based methods. In addition to that bimetallic ultra small nanoparticles of Pd-Pt combination at around 1nm size had also been successfully synthesized using ultrasonication method[49]. Further the synthesis of NiTi/Ni-TiO_2 composite nanoparticles via ultrasonic has been reported more recently[50].

We have recently reported the ultrasonication based synthesis of curcumin nanoparticles directly from turmeric rhizomes [51]. Although, ultrasonication based methods had been portrayed as efficient ecofriendly methods for the synthesis of various nanomaterials from a variety of sources, it has not been employed to synthesize nanoparticles directly from whole biomass of living organisms. As such, irrespective of prokaryote or eukaryote, the cells are built up with countless nanostructured macromolecules such as protein, DNA etc., In addition to that, there exists numerous nano cavities/spaces in between molecules which could possibly provide a nanocarrier platform for a wide variety of molecules as it contains many positive/negatively charged, hydrophilic/hydrophobic regions.

Therefore in this present study, we have focused on the synthesis of nanoparticles directly from *E.coli* using a rapid and simple method by fixing them in glutaraldehyde solution, dehydration in ethanol and probe based ultrasonication method. The resulted particles were separated by differential centrifugation and characterized by UV/Vis, Fluorescent and FTIR spectroscopy and

TEM and confocal microscope. Further the internalization ability of particles has been tested through interaction with Hela cells. The internalization was traced by confocal laser scanning microscope imaging and the biocompatibility established via MTT assay.

Materials and methods

Chemicals

A non- pathogenic *Escherichia coli* (ATCC 11234) was purchased from Korean culture centre of microorganisms, Seoul, South Korea. Glutaraldehyde solution was purchased from Sigma Inc., USA. Ethanol (absolute) was purchased from Merck (Darmstadt, Germany). Nutrient agar medium was purchased from Difco (Detroit, MI, USA). All the chemicals used in the study, unless specified as otherwise, were all of analytical grade. Millipore water was used for all experiments.

Experimental procedures

Culturing of bacteria

A loop full of *E.coli* was spread on a nutrient agar plate and incubated overnight 37^{o}C for the bacterial mat to appear. 100 mg of the bacteria was scooped carefully and transferred to an eppendorf tube and used for bacterial nanoparticles synthesis. The bacteria in the tube were treated with glutaraldehyde solution (5% v/v) in distilled water for 4 hours and then the solution was removed by centrifugation at 8000 rpm for 10 min. After the removal of the supernatant, the bacterial pellet was washed with distilled water and passed through series of ethanol changes (25, 50, 75 100 and 100%) for 15 min each. The excess ethanol was decanted and the cells were

dispersed in 1 mL distilled water (control) and the other set, in 1 mL distilled water containing acridine orange (0.001% w/v).

Nanoparticle synthesis

The samples containing bacteria were subjected to probe type sonication using a Bandelin Sonopuls HD 2200 (GmbH & Co. KG, Heinrichstrase, Berlin, Germany) probe ultrasonicator with 200 W ultrasonic power and a frequency of 20 kHz. The samples were sonicated one after another, with the probe directly in contact with the sample solution held in falcon tubes. The particle synthesis was done at 50% (10 kHz frequency) and 100% (20 kHz frequency) sonication frequency (SF) respectively with different sonication time durations such as 3 min and 5 min. The samples were then stirred for 2 hours in a MS-3000, high speed magnetic stirrer (Mtop inc., South Korea). The solution was centrifuged at 5000, 8000 rpm for five min and subsequently 20000 rpm for 30 min to separate different sized particles. The particles obtained were washed 4 times and re-suspended in a known volume of distilled water.

Characterization

The particles obtained at optimum sonication power were characterized using a UV/Vis spectrophotometer (Nanodrop *ND*-1000 v 3.3.1 spectrophotometer, Nanodrop Technologies, Inc., Wilmington, USA) and FTIR analysis (Shimadzu FTIR-8300 spectrometer, San Diego, CA, USA). Further, the loading of acridine orange into the particle was confirmed by measuring the fluorescent emission at 400 nm using a Fluorescent spectrometer (Hitachi, F-2700, Hitachi, High Technologies America Inc., USA) operating on FL solutions version 4.1 software. Transmission electron micrographs of the particles were obtained using Carl Zeiss LIBRA 120 transmission electron microscope (Carl Zeiss Inc., Oberkochen, Germany) at 120 kV by

depositing the aqueous solution containing separated particles on a copper grid separately with the help of a micropipette, and then kept overnight in a vacuum drying oven (Biofree Inc., South korea). The size distribution of the particles from TEM micrographs were calculated using OPTIMAS 6.1 (Optimas corporation, Langham Creek, Houston, TX, USA). For the elemental composition analysis, the nanosized particles were prepared by placing them on silica coated on aluminum sheets and coated with platinum (for electrical conduction) before the analysis in FE-SEM. The elemental composition analysis and further elemental mapping of the nanosized particles were carried out in FE-SEM (Carl Zeiss, SUPRA® 55 with GEMINI®) using Energy Dispersive X-rays Analysis (EDAX or Energy Dispersive Spectroscopy, EDS).

Particles shapes and the fluorescence emission were characterized using confocal laser scanning microscope (CLSM), (Olympus FluoView™ FV1000 (Olympus America INC., NY, USA).

Cellular imaging

Hela cells (1×10^4) were cultured in DMEM supplemented with 10% FBS in a 26-well tissue culture plates for 12 h at 37^o C in a humidified incubator supplied with 5% CO_2. After growth, the aspirated media was removed and the fresh medium containing three different concentrations of 5, 50 and 100µg particles (with different size and shape) were replaced with the cells. The cells were allowed to grow for 6 h. Then the media was removed and the cells were washed with PBS solution and fixed with paraformaldehyde solution (2% v/v in PBS). The particles treated cells were observed under Confocal laser scanning microscope (CLSM), (Olympus FluoView™ FV1000, Olympus America Inc. NY, USA), for the uptake of particles by Hela cells.

Evaluating cell viability using MTT assay

To quantify the effect of the three different particles on cell viability of Hela cells, an MTT (3-(4,5-dimethyl-thiazol-2-yl)-2,5-diphenyl tetrazoliumbromide) assay was conducted. After the cells were treated using three different sized particles for 12 h, the medium was carefully removed, washed gently using PBS and incubated with 0.5 mg/ml of 3-(4,5-dimethyl-thiazol-2-yl)-2,5-diphenyl tetrazoliumbromide (MTT) (Sigma Chemical Co., St. Louis, MO) in complete DMEM medium for 3 h. The live cells converted MTT to formazan (blue-purple color) when dissolved in dimethyl sulfoxide (DMSO). The intensity of formazan was measured at 570 nm using a plate reader (Multiskan GO-Thermo Scientific Inc., USA) for enzyme-linked immunosorbent assays. Cell viability was calculated by dividing the absorbance of the cells treated with particles/laser by that of untreated cells.

Results and discussion

Fig. 1 shows the successful synthesis of nanoparticles from glutaraldehyde fixed bacterial biomass by using eco friendly ultrasonication method. The bacterial cells were collected, fixed with glutaraldehyde, dehydrated with ethanol and sonicated using ulrasonication probe. During these processes, it is understood that the ultrastructural details of bacterial biomass are preserved and when those cells are subjected for ultrasonication, it resulted in particles of various sizes including nanosized particles. In this study, we have taken colonies of *E. coli* and ultrasonicated them at 50 and 100% sonication power for 3 and 5 min after fixation and dehydration with 5% glutaraldehyde and ethanol respectively. Fig. 2 and 3 shows the TEM micrograph of particles of bacterial origin after various sonication conditions that were separated by applying differential centrifugation forces. After treating the cells with 50% sonication power for 3 minutes, the particles from the supernatant were separated by differential centrifugation. We have observed

that micrometer sized intact cellular structures and broken cells predominated in the pellet separated at 5000 rpm centrifugal force (Fig. 2 a, b; Fig S1 a,,b). Further consecutive centrifugation of supernatant at 8000 rpm resulted in particles sizes (Fig S2 a,b) lesser than the cellular debris and aggregated in the polysaccharide like matrix (Fig. 2c,d). The duration of sonication had shown least impact on the structure of the particles separated by applying 5000 and 8000 rpm centrifugal force (Fig 2a and 2b; Fig 2c and 2d respectively). Further centrifugation of the supernatant at 20000 rpm, resulted in spherical shaped nanosized particles with different sizes. The nano particles obtained from the 3 minutes sonicated samples lie in the size between 8-33nm (Table S1) and it was found to be between 33-42 nm upon 5 min sonication (Fig. 2e, f; Table S1). Sonication timing had a profound influence on the nanoparticles morphology. At 3 min sonication, the particles appeared as irregularly spheres whereas the extension of sonication to 5 min resulted in well defined spherical shaped particles (Fig. 2e, f). We have also applied 100% sonication power for 3 and 5 minutes and subjected the solution for centrifugation at 8000 rpm to remove all the debris and microsized particles. The nanosized particles from the supernatant were separated at 20000 rpm and compared with the nanosized particles obtained from 50% sonication power (Fig. 3). Out of four different variables such as sonication energy (50, 100%) and sonication timing (3 and 5 min) tested, we found that nanoparticles with a distinct morphology were formed upon 5 min of sonication at 50% energy (Fig 3a-d). The elemental mapping of the nanosized particles is given in Fig. S3 (a-l). The EDS analysis showed the distribution of elements such as carbon (Fig. S3b, d), oxygen (Fig. S3b, e), sodium (Fig. S3b, f), aluminium (Fig. S3b, g), silicon (Fig. S3b, h), chloride (Fig. S3b, i), potassium (Fig. S3b, j), platinum (Fig. S3b, k)and nitrogen (Fig. S3b, l). Among the various elements detected, after subtracting the aluminum, silica and platinum (elements used during

sample process for FESEM analysis), carbon was found to be the most abundant (80.94 weight percentage) and was followed by oxygen (18.29 weight percentage), chloride (0.24 weight percentage), sodium (0.21 weight percentage), Nitrogen (0.17 weight percentage) and potassium (0.15 weight percentage) (Table S2) which are generally found with bacterial cellular components.

It is a well known fact that the bacterial structures are made of proteins, carbohydrates, phospholipids, nucleic acids and other bio molecules. As a matter of fact, these molecules are specially designed nanostructures which are compactly assembled to make organelle structures. Upon molecular assembly, these structures are endowed with ample nanospaces between nanostructures. These flexible cellular bio material nanostructures with nanospaces could be preserved by treating with chemical fixative, glutaraldehyde, to rigid nanostructures. In general, glutaraldehyde reacts with amino groups, sulfhydryl groups and possibly with aromatic ring structures of proteins, phospholipids containing free amino groups, for instance, phosphatidylserine and phosphatidylethanolamine[52-54] and fixes them as rigid structures.

Ultrasonic based methods have proved to be highly efficient for the successful synthesis of nanoparticles of metals [58, 59], carbides, sulfides[60] and even some molecules of organic origin[54, 60]. Although, this technique has been followed for the preparation of some nanoparticles, it has not been used for the synthesis of nanoparticles directly from bacterial biomass as was achieved in the present study (Fig. 3b). This is advantageous over other nanoparticles since it can be used to load molecules and therefore it could serve as an efficient platform for drug delivery system. To

ensure the holding capacity of nanoparticles for molecules and to trace their cellular uptake, the nanoparticles were intercalated with acridine orange and characterized by UV-Vis (Fig. 4a), fluorescence (Fig. 4b) and FTIR (Fig. 4c) spectroscopy and confocal imaging (Fig. S4 a-i).

As evidenced from the UV Vis spectra, the particles separated at 5000 rpm exhibited high absorbance property than the particles obtained at 20000 rpm (Fig. 4a). Maximum absorption at 450-550 nm of the particles synthesized with acridine orange confirms the loading of acridine orange in the particles whereas the particles synthesized in the absence of AO completely lack the absorption at 450-550 nm (corresponding absorption of AO). This confirms the proper loading of dye in the particle (Fig. 4a). Unlike the control particles, the fluorescence emission of particles at around 540-550 nm confirms the loading of AO into the particles and the shift in the emission maxima from 550 nm for the particles obtained at 5000 rpm (5391 a.u) and 8000 rpm (4419 a.u) to 546 nm for the particles obtained at 20000 rpm (3792 a.u) clearly denotes the changes in the particle size (Fig. 4b). Fig. 4c confirms the positive AO loading on nanoparticles obtained at high speed centrifugation by FTIR spectrum. A peak at 1052 cm^{-1} (marked as 3 in Fig. 4c) is observed in AO treated NPs which is attributed to the C-N stretching vibrations of AO, in which, the free amine groups at the end of this molecule may bound to the NPs leading to the formation of secondary amines. Apart from this, there is a broad peak at 1280 cm^{-1} (marked as 2 in Fig 4c) which is ascribed to the C-N stretching vibrations of AO that might have arisen from the primary amines of AO in its unbounded form. Green fluorescence emission of the three different AO loaded particles separated by differential centrifugation was qualitatively verified by confocal imaging and all the three particles exhibited the green fluorescence confirming the loading of AO in particles (Fig S4 a-i).

In order to study the cellular internalization ability of all the three different particles synthesized by the sonication based method, 5, 50 and 100µg particles were treated with Hela cells for 6 hours and observed by confocal laser scanning microscope (Fig. 5). Out of the 3 particles tested, the internalization ability of the nanosized particles obtained at high centrifugal force (20000 rpm) was found to be highest (fig 5a-c) than the other two particles obtained at 5000 rpm (Fig. 5d-f) and 8000 rpm (Fig 5g-i) respectively. Through this study it is proved that these particles could be used as efficient drug carriers. In general, due to the increase in the surface to volume ratio, it is so obvious that the nanoparticles can be loaded with more molecules on its surface than their core counterparts[59]. In addition to that the diffusion distance is reduced for the nanoparticles than the microsized particles for cellular application[60]. The size and shape effect of the metallic and polymeric nanoparticles on the internalization abilities had been in the past studied with different cell lines. Chitrani et al.,[61] had treated different sized gold nanomaterials (between 14 and 100 nm) with Hela cells and had found that spherical shaped nanoparticles around 50nm size exhibited a maximum internalization potential. Further research has shown that the best size for improved uptake of spherical shaped nanoparticles was around 25-30nm[62-64] and they had identified that the nanoparticles uptake mechanism for most of the spherical shaped nanoparticles was operated through receptor-mediated endocytosis. The Hela cells in the present study also showed maximum uptake of the nanoparticles with 33 to 42 nm size, and therefore it is presumed that the particles could have been taken up into the Hela cells through the receptor-mediated endocytosis process. We speculate that the nanoparticles system synthesized directly from biomass is composed of a network of nanosized molecules which harbor increased nano surfaces, and therefore we consider the present system more superior than the other drug delivery systems.

After the treatment of cells with three different particles, their effect on the cell viability was evaluated using MMT assay. Fig. S5 gives the percentage of the viable cells obtained by MTT assay subsequent to treatment. As can be observed, only <5% of the cells were affected subsequent to treatment using high concentration (100µg) of nanosized particles. The other particles obtained at 5000 and 8000 rpm resulted only up to 2% cell death. Although the nanosized particles were more internalized, with and without AO, the killing effect of those particles was very limited and therefore it is quite clear that they exhibit extreme biocompatibility and would undoubtedly act as excelling platforms as drug carriers.

Acknowledgement

This work was supported by the KU Research Professor Program of Konkuk University,

References

1. G. Schmid, Nanoparticles: From Theory to Application Edited by Günter Schmid. Wiley–VCH, 2004, pp611

2. T. Tsuzuki, Int. *J. Nanotechnol*., 2009, 6(5/6), 567 - 578

3. J. Perez, L. Bax, and C. Escolano, C. Roadmap, Report on Nanoparticles, 2005, Willems & van den Wildenberg, Spain.

4. R. Kessler, Engineered Nanoparticles in Consumer Products. *Environ. Health Persp*., 2011, 119 (3), A120-A125

5. L. Calzolai, D. Gilliland and F. Rossi, Food Addit. Contam. Part A, 2012, 29 (8), 1183–1193

6. T.A.Taton, *Trends Biotechnol*., 2002, 20, 277-279.

7. O,V. Salata, *J. Nanobiotech*., 2004, 2, 1-6.

8. M. Bruchez, M. Moronne, P.Gin, S. Weiss, A.P. Alivisatos, *Science*, 1998, 281, 2013-2016.

9. W.C.W. Chan, S.M. Nie, *Science* 1998, 281, 2016-2018.

10. S. Wang, N. Mamedova, N.A. Kotov, W. Chen, J. Studer, *Nano Letters,* 2002, **2:**817-822.

11. C. Mah, I. Zolotukhin, T.J. Fraites, J. Dobson, C. Batich , B.J. Byrne, *Mol .Therapy,* 2000, 1, S239-S242.

12. D. Panatarotto, C.D. Prtidos, J. Hoebeke, F. Brown, E. Kramer, J.P. Briand, S. Muller, M. Prato, A. Bianco, *Chem. Biol.,* 2003, 10, 961-966.

13. R.L.Edelstein, C.R. Tamanaha, P.E. Sheehan, M.M. Miller, D.R. Baselt, L.J.Whitman, R.J. Colton, *Biosensors Bioelectron.,* 2000, 14, 805-813.

14. J.M. Nam, C.C.Thaxton, C.A. Mirkin, *Science,* 2003, 301, 1884-1886.

15. R. Mahtab, J.P. Rogers, C.J. Murphy, *J. Am. Chem. Soc.,* 1995, 117, 9099-9100.

16. J. Ma, H. Wong, L.B. Kong, K.W. Peng, *Nanotechnol.,* 2003, 14, 619-623.

17. A. de la Isla, W. Brostow, B. Bujard, M. Estevez, J.R. Rodriguez, S. Vargas, V.M. Castano, *Mat. Resr. Innovat.,* 2003, 7, 110-114.

18. J. Yoshida, T. Kobayashi, *J. Magn. Magn. Mater.,* 1999, 194,176-184.

19. M.Manikndan, N. Hassan, H. F. Wu, *Biomaterials*, 2013, 34(23):5833-42

20. R.S. Molday, D. MacKenzie, *J. Immunol. Methods,* 1982, 52, 353-367.

21. R. Weissleder, G. Elizondo, J. Wittenburg, C.A. Rabito, H.H. Bengele, L. Josephson, *Radiology,* 1990, 175, 489-493.

22. W.J. Parak, R. Boudreau, M.L. Gros, D. Gerion, D. Zanchet, C.M. Micheel, S.C. Williams, A.P. Alivisatos, C.A. Larabell, *Adv. Mater,* 2002, 14, 882-885.

23. S. Andreescu, M. Ornatska, J.S. Erlichman, A. Estevez, J.C. Leiter, Fine Particles in Medicine and Pharmacy, Matijević**,** Egon (Ed.) 2012, pp 57-100

24. P.C. Lee, D. Meisel, *J. Phys. Chem.,* 1982, 86(17), 3391–3395.

25. J.A. Creighton, C.G. Blatchford, M.G. Albrecht, Mol. Chem. Phys., 1979, 75(5), 790–798.

26. L. Longenberger, G. Mills, *J. Phys. Chem.* 1995, 99(2), 475–480.

27. S. Panigrahi, S. Kundu, S. K. Ghosh, S. Nath, T. Pal, *J. Nanoparticle Res.,* 2004, 6:411–414

28. K.S. Suslick, S.B. Choe, A.A. Cichowlas, M.W. Geenstaff, *Nature*, 1991, 353*,* 414.

29. M.S. Wu, Y.H. Ou, Y.P. Lin, *J. Electrochem. Soc.* 2011, 158, 231.

30. C.I. Wu, J.W. Huang, Y.L. Wen, S.B. Wen, Y.H. Shen, M.Y. Yeh, *Materials Lett.* 2008, 62, 1923.

31. M.A.L. Quintela, *Curr. Opin. Coll. Int. Sci.,* 2003, 8, 137.

32. M.C. Advincula, F.G. Rahemtulla, R.C. Advincula, E.T. Ada, J.E. Lemons, S.L. *Biomaterials*, 2006, 27, 2201.

33. B.S. Kwak, B.H. Choi, M.J. Ji, S.M. Park, M. Kang, *J. Ind. Eng. Chem*., 2012, 18, 11.

34. C. B Murray, D. J Norris, M. G Bawendi. J Am Chem Soc. 1993, 115, 8706.

35. T. J Trentler, T. E Denler, J. F Bertone, A. Agrawal, V. L Colvin. *J. Am. Chem. Soc*.,1999, 121, 1613.

36. M. Green, P. O'Brien. *Chem. Commun.,* 2000, 183-184.

37. S. Horikoshi, N. Serpone, Nanoparticle Synthesis—Fundamentals and Applications, Wiley-VCH, Weinheim, Germany, 2013.

38. L Rinaldi, D. Carnaroglio, D. Rotolo, G. Cravotto. *J. Chem.,* 2015, Article ID 879531, 1-8 http://dx.doi.org/10.1155/2015/879531

39. U. K. Parashar, S. P. Saxena, A. Srivastava, *Digest J. Nanomater. and Biostruct.,* 2009, 4(1), 159- 166.

40. K.N. Thakkar, S. S. Mhatre, and R.Y. Parikh, *Nanomed.,* 2010, 6, 257–262

41. M.C. Edmundson, M. Capeness and L. Horsfall, , New Biotechnol., 2014, 31(6) 572-578.

42. P. Golinska, M. Wypij, A. P. Ingle, I. Gupta, H. Dahm, M. Rai, *Appl. Microbiol. Biotechnol.* 2014, 98 (19), 8083-8097

43. J. Athinarayanan, V. S. Periasamy, M. Alhazmi, K. A. Alatiah, A. A. Alshatwi, *Ceramics International*, 2015, 41(1) Part A, 275–281

44. J. H. Bang, K. S. Suslick, *Adv. Mater*. 2010, 22, 1039–1059

45. I. A. Wani, A. Ganguly, J. Ahmed, T. Ahmad, *Mater. Lett.*, 2011, 65(3) 520–522

46. Y. Han, L. L. Zhang, L. Han and S. Dong, *J. Mater. Chem. A*, 2015, DOI: 10.1039/C5TA03090K

47. X. Qian, W. Wang, W. Kong, Y. Chen, *J. Nanomater*. 2014, Article ID 972475, 1-8 pages http://dx.doi.org/10.1155/2014/972475

48. Y. Han, L. Han, L. Zhang, S. and Dong, *J. Mater. Chem. A*, 2015, 3, 14669-14674

49. S. Shafii , W. Lihua, M.R. Nordin, L.K.Yong, J. Chem. Eng. Process Technol. 2012, 3:123. doi: 10.4172/2157-7048.1000123

50. P. Majeri, R. Rudolf, I. Anel, J. Bogovi, S. Stopi, B. Friedrich. Mater. Technol. 2015, 49, 1, 75–80

51. J. Gopal, M. Manikandan, C. Sechul, *RSC advances.,* 2015, 5, 48391-48398

52. L. Paljarvi, J.H. Garcia, H. Kalimo, *Histochem. J.,* 1979, **11**: 267-276.

53. S.E. Ruzin, *Plant Microtechnique and Microscopy*. New York: Oxford University Press. (1999).

54. J.A. Kiernan, *Microscopy Today*, 2000, 00-1, 8-12.

55. Okitsu, Y. Mizukoshi, H. Bandow, Y. Maeda, T. Yamamoto, Y. Nagata, *Sonochem.,* 1996, 3, 249-251.

56. T. Hyeon, M. Fang, K.S. Suslick, J. *Am. Chem. Soc.,* 1996, 118**,** 5492-5493

57. G.S. Wu, X.Y. Yuan, *J. Mat. Lett.*. 2004, 58, 794–797.

58. M.H. Sadr, H. Nabipour, *J. Nanostruct. Chem.,* 2013, 3:26

59. H.M. Redhead, S.S. Davis, L. Illum. *J. Control. Release,* 2001, 70, 353–363

60. H. Yue, W. Wei, Z.G. Yue, P.P. Lv, L.Y. Wang, G.H. Ma, Z. Su, *Eur. J. Pharm. Sci.,* 2010, 41, 650–657

61. B.D. Chithrani, A.A. Ghazani, W.C.W. Chan, Nano Lett., 2006, 6(4), 662–668

62. H. J. Gao, W. D. Shi, L. B. Freund, Proc. Natl. Acad. Sci. USA, 2005, 102, 9469-9474.

63. Y. Aoyama, T. Kanamori, T. Nakai, T. Sasaki, S. Horiuchi, S. Sando, T.Niidome, J. Am. Chem. Soc. 2003, 125, 3455-3457.

64. B. D. Chithrani, W. C. W. Chan, Nano Lett. 2007, 7, 1542-1550

Figure captions

Fig. 1 Schematic of experimental design of the study showing sample collection, pretreatment for ultrasound based nanoparticles synthesis and application of particles for cellular uptake.

Fig. 2. TEM images of particles synthesized from bacterial biomass by ultrasonication (50% sonication power) at different timings and separated using different centrifugation speed. (a) 3 min and 5000 rpm; (b) 5 min and 5000 rpm; (c) 3 min and 8000 rpm; (d) 5 min and 8000 rpm; (e) 3 min and 20000 rpm; (f) 5 min and 20000 rpm.

Fig. 3. TEM images of nanoparticles synthesized from bacterial biomass by ultrasonication and separated by centrifugation at 20000 rpm after removal of microsized particles by consecutive centrifugation at 5000 and 8000 rpm. (a) 3 min at 50% sonication power; (b) 5 min at 50% sonication power; (c) 3 min at 100% sonication power; (d) 5 min at 100% sonication power.

Fig. 4. Characterization of particles synthesized from bacterial biomass by ultrasonication method. (a) UV/Visible spectrum of particles; (b) Fluorescence emission (excitation at 270 nm) spectrum (c) FTIR spectrum of particles. (5K-5000 rpm; 8K-8000 rpm; 20K- 20000 rpm)

Fig. 5. Probing the internalization ability of different sized particles synthesized from bacterial biomass by ultrasonication (50% sonication power for 5 min) into Hela cells by Confocal laser scanning microscopic images after treating the cells with particles for 6 hours. (a-c) internalization of particles obtained at 5000 rpm; (d-f) internalization of particles obtained at 8000 rpm; (g-i) internalization of particles obtained at 20000 rpm (scale bar - 20μm)

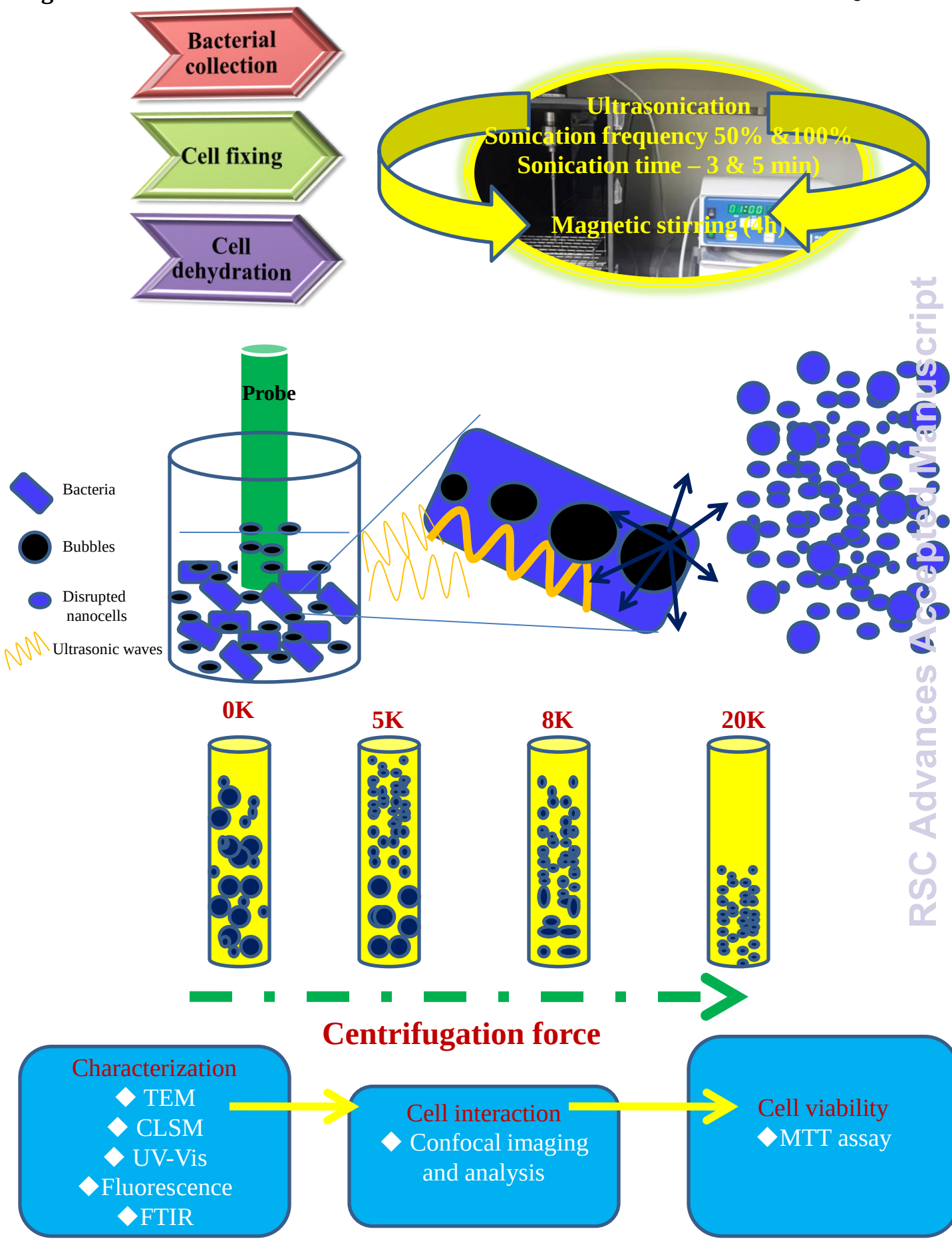

Fig. 2

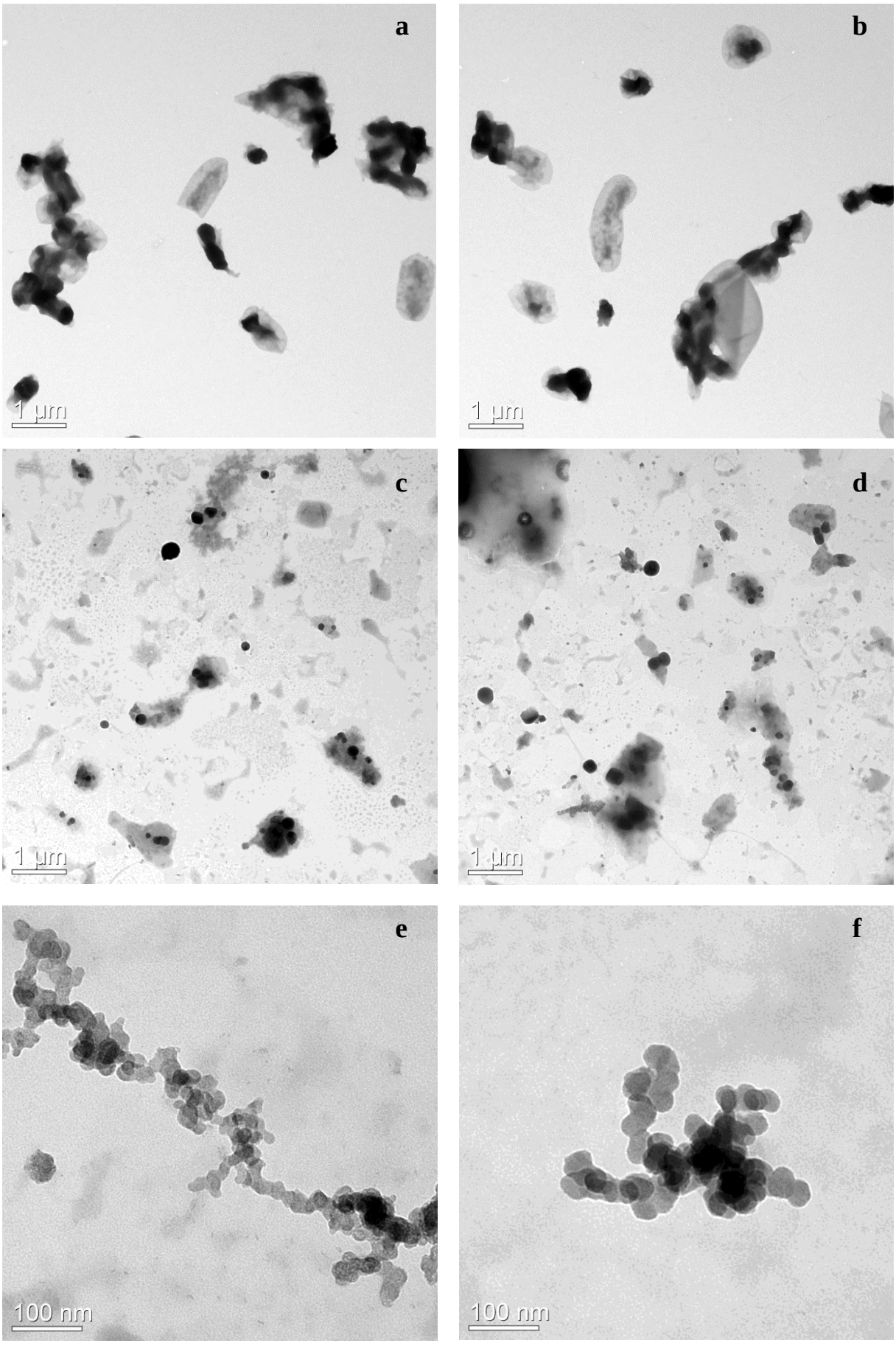

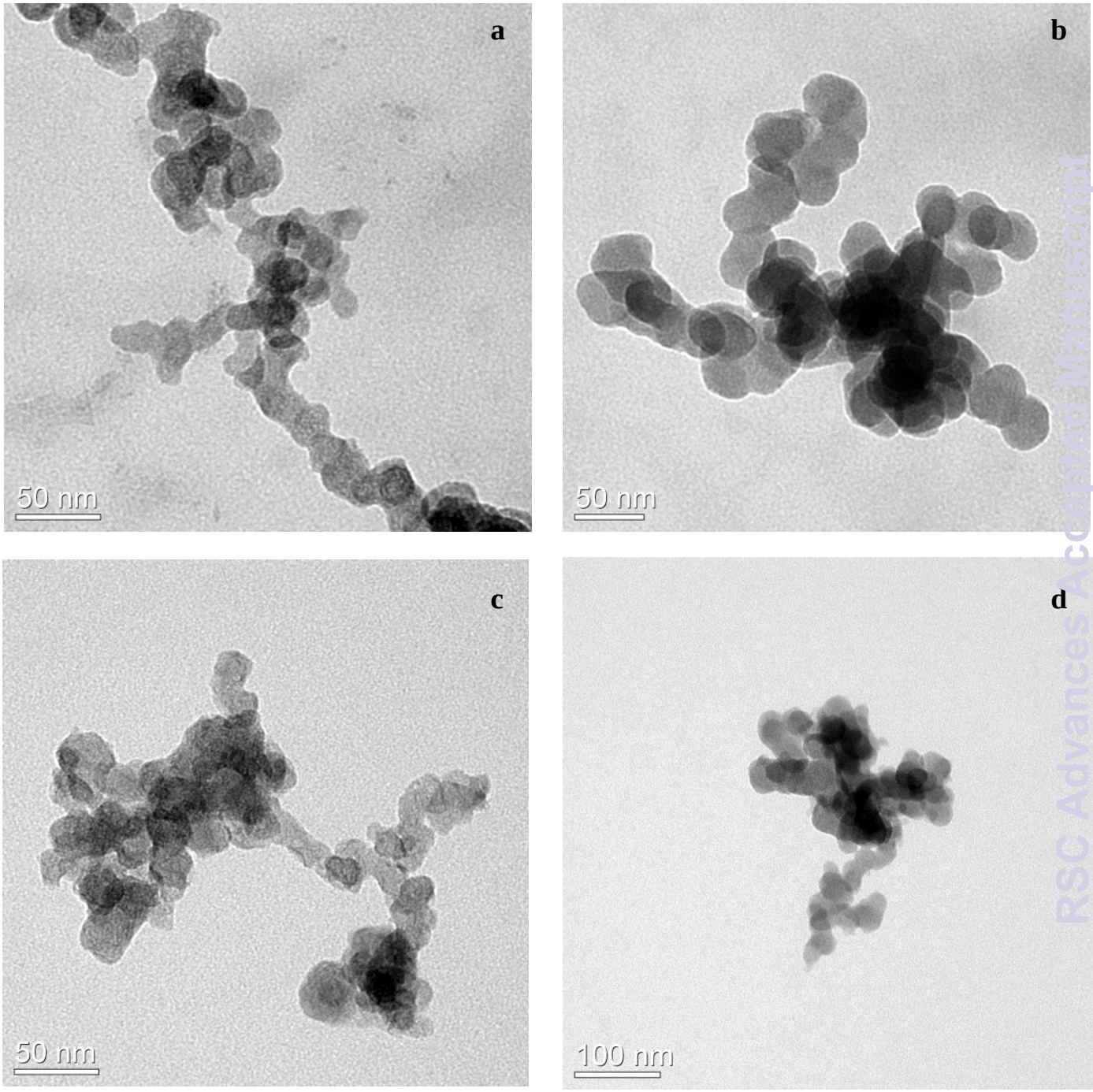

Fig. 4